FERMIONS SCATTERING ON FEW IMPURITIES: FRIEDEL OSCILLATIONS AND HUYGENS SUPERPOSITION PRINCIPLE*

Jan Skolimowski

International Research Centre MagTop
Institute of Physics, Polish Academy of Sciences
Aleja Lotników 32/46, 02-668 Warszawa, Poland

Banhi Chatterjee

Fakultät für Physik and CENIDE, Universität Duisburg-Essen
Lotharstr. 1, 47057 Duisburg, Germany

Krzysztof Byczuk

Institute of Theoretical Physics, Faculty of Physics, University of Warsaw
Pasteura 5, 02-093 Warszawa, Poland

Received 5 February 2026, accepted 16 March 2026, published online 15 May 2026

The Friedel formula describing oscillations of the electron density due to the presence of a single impurity has been known for a long time. Here, we derive a generalized formula for the case of many impurities and we discuss in detail specific cases where few scattering centers are present. Interference patterns in the density oscillations are shown. The arguments are presented when the standard Friedel's formula can be used additively and the inter impurity scatterings might be neglected. One can view our result as the Huygens principle applied to Friedel oscillations in many impurity cases.

DOI:10.5506/APhysPolB.57.5-A6

1. Introduction

The Friedel formula [1, 2]

$$n(\boldsymbol{r}) = n_0 + A\frac{\cos(2k_{\mathrm{F}}r + \phi)}{r^d} \tag{1}$$

* Presented at the Concepts in Strongly Correlated Quantum Matter Conference (CSCQM), Kraków, Poland, 20–22 November, 2025.

is one of the best recognized results in solid state physics and quoted in many textbooks, *e.g.* [3]. It describes how the density of free electrons $n(\boldsymbol{r})$ oscillates with the distance r far away from the localized impurity potential in a d-dimensional system with the Fermi vector length k_{F} at zero temperature. A phase shift is denoted by ϕ and an amplitude constant is given by A. On top of the algebraic, universal power-law decay of the density variation with respect to the uniform case n_0, *i.e.* without the impurity, there are Friedel oscillations (FO) due to the Pauli exclusion principle obeyed by fermions. The observation of FO in material systems is a direct confirmation of quantum mechanics principles putting the Friedel formula on a pedestal of the most important equations in physics.

Original motivation of Jacque Friedel's works [1, 2] was to understand metallic alloys; for more information, see recent reviews: [4–7]. The invention of scanning tunelling microscopy (STM) [8, 9] made a direct observation of FOs possible [10–13]. Indeed, FOs were seen in various metals and semiconductors, *e.g.*, on surfaces Cu(111), GaAs(111), or Si(111)Ag [10, 14, 15].

In particular, in quantum corrals [11–13, 16], the electron wave function is scattered on a finite number of impurities arranged in some geometric pattern. It is therefore a naturally interesting question how, if any, formula (1) can be used to describe such systems where interference patterns due to scattering on many centers play an important role.

As a matter of fact, the STM-like experiments map FO directly in the local density of states (LDOS) on probed surfaces [9]. To obtain FO in density of particles at zero temperature, one needs to integrate the LDOS up to the Fermi level. Nevertheless, the oscillations in the LDOS and in the density are of the same origin.

In this paper, we revisit the problem of multiple scattering theory, see *e.g.* [16], and analyze it in the case of a small number of scattering centers. We show directly that if the distance between impurities is large, one can follow a kind of Huygens principle and describe the interference pattern by summing the Friedel oscillations (1) from each impurity potential separately. This Huygens generalization of the Friedel result to a few impurity problems has not been discussed in detail yet. If distances between impurities or the observation point from scattering centers are small, the multiple scattering interference effects should be taken into account via off-diagonal elements of the t-matrix.

2. Exact formal solution

Our non-interacting system is described by the one-particle Green's function [17]

$$G\left(\boldsymbol{r},\boldsymbol{r}';\omega\right)=\langle\boldsymbol{r}|\frac{\hbar}{\hbar\omega-\hat{H}}|\boldsymbol{r}'\rangle\,, \tag{2}$$

where $\hbar\omega$ is the real energy ($\hbar$ is the Planck constant) and the one-particle Hamiltonian $\hat{H}$ is given by

$$\hat{H}=-\frac{\hbar^2}{2m}\nabla^2+V(\boldsymbol{r})\,, \tag{3}$$

which contains an external potential

$$V(\boldsymbol{r})=\sum_{i=1}^{N_{\rm imp}}\tilde{V}_i(\boldsymbol{r}-\boldsymbol{l}_i)\,, \tag{4}$$

originated from $N_{\rm imp}$-independent impurities located at positions $\boldsymbol{l}_i$, with $i=1,2,\ldots,N_{\rm imp}$. The vector $\boldsymbol{r}$ is the particle position variable and m is its mass. All d-dimensional vectors are denoted in boldface. It is known that the one-particle Green's function in the presence of an external potential $V(\boldsymbol{r})$ obeys an integral (Dyson) equation [17]

$$G\left(\boldsymbol{r},\boldsymbol{r}';\omega\right)=G_0\left(\boldsymbol{r}-\boldsymbol{r}';\omega\right)+\int{\rm d}r''G_0\left(\boldsymbol{r}-\boldsymbol{r}'';\omega\right)V\left(\boldsymbol{r}''\right)G\left(\boldsymbol{r}'',\boldsymbol{r}';\omega\right)\,, \tag{5}$$

where $G_0(\boldsymbol{r}-\boldsymbol{r}';\omega)$ is the free one-particle Green's function, *i.e.* with $V(\boldsymbol{r})=0$. In the $d=2$ and $d=3$ dimensions, it takes the explicit form [17]

$$G_0\left(\boldsymbol{r}-\boldsymbol{r}';\omega\right)=\begin{cases}-\frac{2m}{\hbar^2}\frac{i}{4}H_0^+\left(k|\boldsymbol{r}-\boldsymbol{r}'|\right) & \text{for}\quad d=2\,,\\ -\frac{2m}{\hbar^2}\frac{{\rm e}^{ik|\boldsymbol{r}-\boldsymbol{r}'|}}{4\pi|\boldsymbol{r}-\boldsymbol{r}'|} & \text{for}\quad d=3\,,\end{cases} \tag{6}$$

where $k\equiv k(\omega)=\sqrt{2m\omega/\hbar}$ and $H_0^+(k|\boldsymbol{r}-\boldsymbol{r}'|)$ is the $0^{\rm th}$ order of the first kind Hankel function [18]. We note that the one-particle Green's functions $G_0(\boldsymbol{r}-\boldsymbol{r}';\omega)$ in empty space are singular when $|\boldsymbol{r}-\boldsymbol{r}'|\to 0$. In $d=2$, this singular behavior is logarithmic [18]. Here and in the following, we consider the retarded (out-going) boundary condition, which implies that everywhere ω is replaced by $\omega+i0^+$, where $i0^+$ is an infinitesimally small imaginary constant.

Typically, the impurity potentials $\tilde{V}_i(\boldsymbol{r})$ in Eq. (4) are screened and short range. Therefore, we model them by a zero-range pseudo-potential represented by a Dirac-delta distribution function with the proportionality constant represented by the effective scattering strength $a_i^{\rm scatt}=V_iL^d$, where L

is some characteristic length and V_i is the impurity potential strength. However, such an extremely localized and singular potential must be properly regularized giving rise to the Fermi pseudo-potential [19–23].

In the following, we write

$$V(\boldsymbol{r}) = \sum_{i=1}^{N_{\mathrm{imp}}} a_i^{\mathrm{scatt}} \delta(\boldsymbol{r} - \boldsymbol{l}_i)\,, \tag{7}$$

and the one-particle Green's function $G_0(\mathbf{0};\omega)$ are supposed to be adequately renormalized quantities [20–22]. In particular, in odd dimensions, it is enough to start with the one-particle Green's function in the time domain

$$\tilde{G}_0\left(\boldsymbol{r} - \boldsymbol{r}';t\right) = \left(\frac{m}{2\pi i\hbar t}\right)^{d/2} \mathrm{e}^{\frac{i}{\hbar}\frac{m(\boldsymbol{r}-\boldsymbol{r}')^2}{2t}}\,, \tag{8}$$

which is a Gaussian propagator with $t > 0$ and is regular in the $|\boldsymbol{r} - \boldsymbol{r}'| \to 0$ limit. To derive $G_0(\boldsymbol{r} - \boldsymbol{r}';\omega)$ when $|\boldsymbol{r} - \boldsymbol{r}'| \to 0$, we firstly find $\tilde{G}_0(\mathbf{0};t)$ and then take the Fourier transform to obtain $G_0(\mathbf{0};\omega)$ [20]. In $d = 3$, we get explicitly $G_0(\mathbf{0};\omega) = -2\sqrt{\pi}(m/2\pi\hbar^2 i)^{3/2}\sqrt{\omega}$. The $d = 2$ needs the dimensional regularization $d = 2 - \epsilon$ with $\epsilon \to 0$ and the final result is explicitly given in [20].

For a system with impurity pseudo-potentials (7), the integral equation reads

$$G\left(\boldsymbol{r},\boldsymbol{r}';\omega\right) = G_0\left(\boldsymbol{r} - \boldsymbol{r}';\omega\right) + \sum_{i=1}^{N_{\mathrm{imp}}} V_i G_0\left(\boldsymbol{r} - \boldsymbol{l}_i;\omega\right) G\left(\boldsymbol{l}_i,\boldsymbol{r}';\omega\right)\,. \tag{9}$$

Expressing the left-hand side at $\boldsymbol{r} = \boldsymbol{l}_i$, we obtain a set of linear equations to determine $G(\boldsymbol{l}_i,\boldsymbol{r}';\omega)$, *i.e.*

$$G\left(\boldsymbol{l}_i,\boldsymbol{r}';\omega\right) = G_0\left(\boldsymbol{l}_i - \boldsymbol{r}';\omega\right) + \sum_{j=1}^{N_{\mathrm{imp}}} V_j G_0\left(\boldsymbol{l}_i - \boldsymbol{l}_j;\omega\right) G\left(\boldsymbol{l}_j,\boldsymbol{r}';\omega\right)\,. \tag{10}$$

This set of equations can be written in a matrix form

$$\sum_{j=1}^{N_{\mathrm{imp}}} M_{ij}(\omega)\, G\left(\boldsymbol{l}_j,\boldsymbol{r}';\omega\right) = G_0\left(\boldsymbol{l}_i - \boldsymbol{r}';\omega\right)\,, \tag{11}$$

where the M matrix is $M_{ij}(\omega) = [\delta_{ij} - V_j G_0(\boldsymbol{l}_i - \boldsymbol{l}_j;\omega)]$. The diagonal elements of this matrix $M_{ii}(\omega) = [1 - V_i G_0(\mathbf{0};\omega)]$ are not singular due to a regularization procedure discussed above and in Refs. [20–22]. Then, by

inverting this matrix, in the absence of bound states, either analytically or numerically for each ω, we find the solution of Eq. (10)

$$G\left(\boldsymbol{l}_i, \boldsymbol{r}'; \omega\right) = \sum_{j=1}^{N_{\text{imp}}} M_{ij}^{-1}(\omega) G_0\left(\boldsymbol{l}_j - \boldsymbol{r}'; \omega\right) . \tag{12}$$

Finally, by using Eq. (9), we determine the exact one-particle Green's function

$$G\left(\boldsymbol{r}, \boldsymbol{r}'; \omega\right) = G_0\left(\boldsymbol{r} - \boldsymbol{r}'; \omega\right) + \sum_{i,j=1}^{N_{\text{imp}}} G_0\left(\boldsymbol{r} - \boldsymbol{l}_i; \omega\right) T_{ij}(\omega) G_0\left(\boldsymbol{l}_j - \boldsymbol{r}'; \omega\right) , \tag{13}$$

where $T_{ij}(\omega) = V_i M_{ij}^{-1}(\omega)$ is a t-matrix.

The LDOS is provided by the diagonal ($\boldsymbol{r} = \boldsymbol{r}'$) part of the one-particle Green's function

$$\rho(\boldsymbol{r}; \omega) = -\frac{1}{\pi} \operatorname{Im} G\left(\boldsymbol{r}, \boldsymbol{r}; \omega\right) , \tag{14}$$

and the local density of non-interacting fermions at $T = 0$ with the Fermi energy E_{F} is given by

$$n(\boldsymbol{r}) = \int_0^{E_{\text{F}}} \mathrm{d}\omega \; \rho(\boldsymbol{r}; \omega) = -\frac{1}{\pi} \int_0^{E_{\text{F}}} \mathrm{d}\omega \; \operatorname{Im} G(\boldsymbol{r}, \boldsymbol{r}; \omega) . \tag{15}$$

It is clear that in the multiple impurity case, the terms $G_0(\boldsymbol{r} - \boldsymbol{l}_i; \omega) G_0(\boldsymbol{l}_j - \boldsymbol{r}; \omega)$ are responsible for an oscillatory behavior with respect to $\boldsymbol{r}$ of the LDOS and the local density. Note that, for simplicity, we neglect the spin of particles, which otherwise would lead to a trivial factor of two in the corresponding equations.

3. Explicit analytical and numerical solutions in special cases

For a small number of scattering centers, one can invert the matrix M analytically and investigate Friedel oscillations in detail.

3.1. A single impurity

For example, for $N_{\text{imp}} = 1$ we find that $M_{11}(\omega) = 1 - V_1 G_0(\mathbf{0}; \omega)$ and therefore

$$G\left(\boldsymbol{r}, \boldsymbol{r}'; \omega\right) = G_0\left(\boldsymbol{r} - \boldsymbol{r}'; \omega\right) + G_0(\boldsymbol{r} - \boldsymbol{l}_1; \omega) T_{11}(\omega) G_0\left(\boldsymbol{l}_1 - \boldsymbol{r}'; \omega\right) , \tag{16}$$

where $T_{11}(\omega) = V_1/(1 - V_1 G_0(\mathbf{0};\omega))$. In Fig. 1 left panel, we present the real and imaginary parts of the t-matrix for the single impurity with $V_1 = 1$ in three dimensions. Herein, we have used units where $2m/\hbar^2 = 1$. The Fermi energy E_F is fixed by demanding that the uniform particle density is equal to one. At $\omega = 0$, the real part of T_{11} approaches a finite value V_1 and its imaginary part vanishes. For a small V_1 parameter, the term $V_1 G_0(\mathbf{0};\omega)$ in the denominator can be neglected and the t-matrix is a real ω-independent constant equal to V_1. This is a weak coupling, linear regime, for which the original Friedel formula (1) was derived. At large V_1, the t-matrix might be approximated by $T_{11}(\omega) = -G_0(\mathbf{0};\omega)^{-1} \sim (-i)^{-3/2}/\sqrt{\omega}$. Apparently, the $V_1 \to \infty$ limit is non-analytical and leads to an unphysical infinitely large imaginary part of T_{11} at zero frequency.

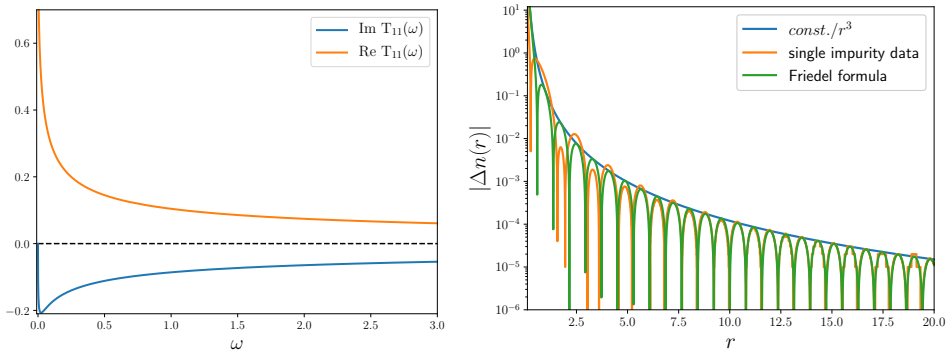

Fig. 1. Left panel: The real and imaginary parts of the t-matrix for a single impurity with $V_1 = 1$. Right panel: Friedel oscillations due to a single impurity with $V_1 = 1$ in three dimensions. The orange curve represents the result determined using the exact t-matrix. The blue curve shows the behavior of the envelope which asymptotically decays with a distance as $1/r^3$ (the constant is 0.15 in this parameter selection). The green curve represents oscillatory behavior derived from the asymptotic Friedel formula (18).

The changes in the local density of particles with respect to the empty space are determined by

$$\Delta n(\boldsymbol{r}) = -\frac{1}{\pi}\int_0^{E_\mathrm{F}} \mathrm{d}\omega\ \mathrm{Im}\, G_0(\boldsymbol{r};\omega) T_{11}(\omega) G_0(-\boldsymbol{r};\omega)\,. \tag{17}$$

In Fig. 1 right panel, we present the exact result for the changes in the particle densities from the potential located at the origin with the vector $\boldsymbol{l} = 0$. The little stepwise behavior at large r is due to a finite numerical accuracy in determining the integrals. It can be easily verified that at large

distances, the amplitudes of the oscillation decay as $1/r^3$, which is described by the original Friedel formula in three dimensions, namely

$$\Delta n(\boldsymbol{r}) = I^{\mathrm{scatt}} \frac{\cos(2k_{\mathrm{F}} r + \phi_s)}{r^3}\,, \tag{18}$$

where I^{scatt} is the constant proportional to the effective scattering length [24]. In deriving Eq. (18), the ω-dependence of the t-matrix is neglected and it is approximated by its value in the $\omega \to 0$ limit, see [24] for details. In Fig. 1 right panel, we plot the density changes determined from the asymptotic Friedel formula (18) and we see that at distances $r > 7$, it practically gives the same results as those obtained exactly.

3.2. Two impurities

For $N_{\mathrm{imp}} = 2$ impurities located at points $\boldsymbol{l}_1$ and $\boldsymbol{l}_2$, we find the explicit solution (13) in the form

$$\begin{aligned} G\left(\boldsymbol{r},\boldsymbol{r}';\omega\right) &= G_0\left(\boldsymbol{r}-\boldsymbol{r}';\omega\right) \\ &+G_0(\boldsymbol{r}-\boldsymbol{l}_1;\omega)T_{11}(\omega)G_0\left(\boldsymbol{l}_1-\boldsymbol{r}';\omega\right) + G_0(\boldsymbol{r}-\boldsymbol{l}_1;\omega)T_{12}(\omega)G_0\left(\boldsymbol{l}_2-\boldsymbol{r}';\omega\right) \\ &+G_0(\boldsymbol{r}-\boldsymbol{l}_2;\omega)T_{21}(\omega)G_0\left(\boldsymbol{l}_1-\boldsymbol{r}';\omega\right) + G_0(\boldsymbol{r}-\boldsymbol{l}_2;\omega)T_{22}(\omega)G_0\left(\boldsymbol{l}_2-\boldsymbol{r}';\omega\right)\,, \end{aligned} \tag{19}$$

where

$$\begin{aligned} T_{11}(\omega) &= \frac{V_1}{[1-V_1G_0(\boldsymbol{0};\omega)][1-V_2G_0(\boldsymbol{0};\omega)]-V_1V_2G_0(\boldsymbol{l}_1-\boldsymbol{l}_2;\omega)G_0(\boldsymbol{l}_2-\boldsymbol{l}_1;\omega)} \\ &\quad\times[1-V_2G_0(\boldsymbol{0};\omega)]\,, \end{aligned} \tag{20}$$

$$\begin{aligned} T_{12}(\omega) &= \frac{V_1}{[1-V_1G_0(\boldsymbol{0};\omega)][1-V_2G_0(\boldsymbol{0};\omega)]-V_1V_2G_0(\boldsymbol{l}_1-\boldsymbol{l}_2;\omega)G_0(\boldsymbol{l}_2-\boldsymbol{l}_1;\omega)} \\ &\quad\times V_2G_0(\boldsymbol{l}_1-\boldsymbol{l}_2;\omega)\,, \end{aligned} \tag{21}$$

$$\begin{aligned} T_{21}(\omega) &= \frac{V_2}{[1-V_1G_0(\boldsymbol{0};\omega)][1-V_2G_0(\boldsymbol{0};\omega)]-V_1V_2G_0(\boldsymbol{l}_1-\boldsymbol{l}_2;\omega)G_0(\boldsymbol{l}_2-\boldsymbol{l}_1;\omega)} \\ &\quad\times V_1G_0(\boldsymbol{l}_2-\boldsymbol{l}_1;\omega)\,, \end{aligned} \tag{22}$$

and

$$\begin{aligned} T_{22}(\omega) &= \frac{V_2}{[1-V_1G_0(\boldsymbol{0};\omega)][1-V_2G_0(\boldsymbol{0};\omega)]-V_1V_2G_0(\boldsymbol{l}_1-\boldsymbol{l}_2;\omega)G_0(\boldsymbol{l}_2-\boldsymbol{l}_1;\omega)} \\ &\quad\times[1-V_1G_0(\boldsymbol{0};\omega)]\,. \end{aligned} \tag{23}$$

Due to the multiple scattering between the two impurities, the t-matrix is not a simple sum of t-matrices for two independent impurities located at

different points. In fact, it is a matrix function whose elements depend on the energy ω and the distance between the impurities $\Delta l = |\boldsymbol{l}_1 - \boldsymbol{l}_2|$. In the limit with $\boldsymbol{l}_1 = \boldsymbol{l}_2$, we obtain the expression for the Green's function $G(\boldsymbol{r}, \boldsymbol{r}'; \omega)$ in the form of Eq. (16) with the total potential $V_1 + V_2$.

In Fig. 2, we plot the real (top panels) and imaginary (bottom panels) parts of the off-diagonal t-matrix elements for different distances between the impurities in three dimensions. For comparison, we also present the ratios of real and imaginary parts between off-diagonal and diagonal matrix elements, respectively. Due to the inter-impurity scattering and interference of quantum waves, the t-matrix oscillates and changes a sign in contrast to the single impurity case as presented in Fig. 1 left panel. Moreover, we can see that with increasing the inter-impurity distance, the relative values of the off-diagonal elements with respect to the diagonal ones are decreasing.

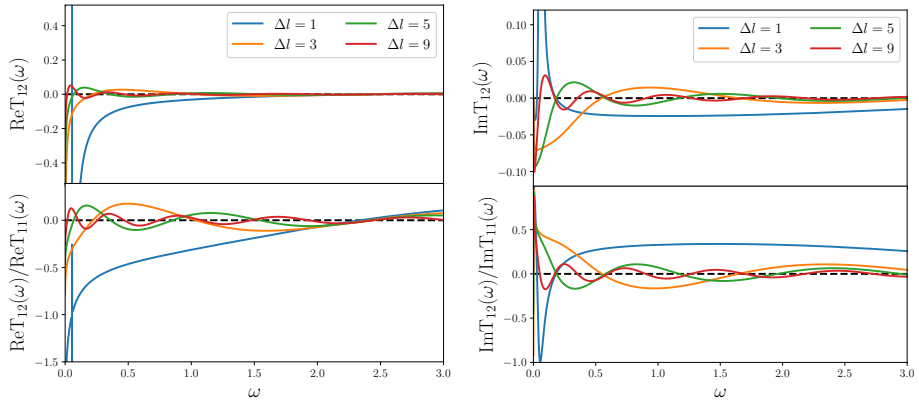

Fig. 2. Real (upper panel) and imaginary (lower panel) of the off-diagonal t-matrix elements and their ratio with respect to diagonal elements for different distances between impurities with $V_1 = V_2 = 1$ in three dimensions.

In Fig. 3, we present exact results for FO in the case of two impurities in three dimensions for different distances Δl. Strong interference oscillations are visible between the impurities. Outside the impurities, the oscillation amplitudes decay as $1/r^3$, similarly as in the one impurity case. In Fig. 3, we also plot the results when the off-diagonal t-matrix elements are not taken into account. Differences are rather small and mostly visible in the space between the impurities. Outside them, the results depicted by blue (exact) and orange (approximate) lines are almost the same. We have checked that with increasing the inter-impurity distance Δl further, the contributions from off-diagonal elements of the t-matrix can be completely neglected. This observation gives rise to an approximate treatment in the next section.

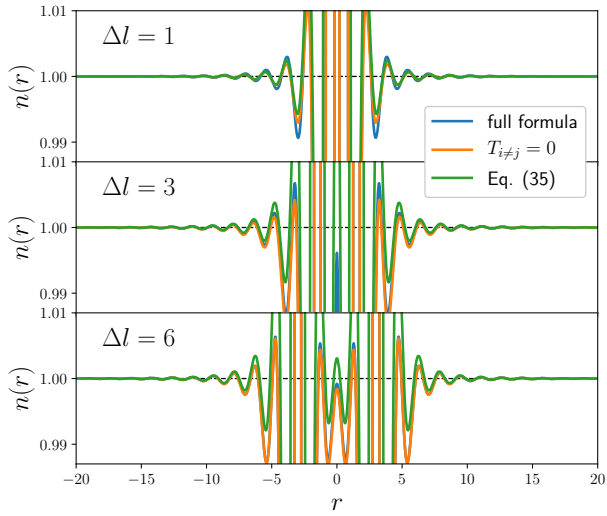

Fig. 3. The Friedel oscillations due to two impurities with $V_1 = V_2 = 1$ at different distances Δl in three dimensions (here, plots are along the axis connecting the two impurities). The blue curves represent the exact result determined using the t-matrix, Eqs. (20)–(23). The orange curves show the behavior of the Friedel oscillations when the off-diagonal elements of the t-matrix are not taken into account. The green curves represent oscillatory behavior derived from the generalized Friedel formula (26).

For $N_{\text{imp}} = 3$ or 4, it is still possible to invert the matrix M analytically and obtain the exact analytical expressions for the one particle's Green's functions. This should also allow us to investigate FO in analytical detail. However, the final equations become more and more cumbersome, *cf.* [21].

4. Approximation in diluted impurity limit and generalized Friedel formula

An important simplification occurs when the impurities are far away from each other, *i.e.*, $|\boldsymbol{l}_i - \boldsymbol{l}_j|$ is large as compared to other relevant distances, *e.g.*, the Fermi wave length. In this diluted limit, we can neglect the off-diagonal elements of the matrix M because the Green's function decays as $G_0(\boldsymbol{l}_i - \boldsymbol{l}_j; \omega) \sim 1/|\boldsymbol{l}_i - \boldsymbol{l}_j|^{(d-1)/2}$, *cf.* Fig. 2 and the discussion in Section 3. In this limit, $M_{ij}^{-1}(\omega) = \delta_{ij}/(1 - V_i G_0(\mathbf{0}; \omega))$ and $T_{ij}(\omega) = \delta_{ij} V_i/(1 - V_i G_0(\mathbf{0}; \omega))$. The t-matrix is diagonal and each matrix element takes into account only multiple scattering off the corresponding single impurity. Inter-impurity scattering effects are neglected in this limit. The one-particle Green's function is now given by $G(\boldsymbol{r}, \boldsymbol{r}'; \omega) = G_0(\boldsymbol{r} - \boldsymbol{r}'; \omega) + \sum_{i=1}^{N_{\text{imp}}} G_0(\boldsymbol{r} -$

$\boldsymbol{l}_i;\omega)T_{ii}(\omega)G_0(\boldsymbol{l}_i-\boldsymbol{r}';\omega)$. The change of the LDOS, due to multiple impurities scatterings, is $\Delta\rho(\boldsymbol{r};\omega)=-\frac{1}{\pi}\sum_{i=1}^{N_{\rm imp}}\mathrm{Im}\,G_0(\boldsymbol{r}-\boldsymbol{l}_i;\omega)T_{ii}(\omega)G_0(\boldsymbol{l}_i-\boldsymbol{r};\omega)$. Finally, the change in the local density is determined from

$$\Delta n(\boldsymbol{r})=-\frac{1}{\pi}\sum_{i=1}^{N_{\rm imp}}\int_0^{E_{\rm F}}\mathrm{d}\omega\;\mathrm{Im}\,G_0(\boldsymbol{r}-\boldsymbol{l}_i;\omega)T_{ii}(\omega)G_0(\boldsymbol{l}_i-\boldsymbol{r};\omega)\,. \tag{24}$$

In the limit of diluted impurities, the FO pattern is a sum of FO patterns coming from each scattering center independently. It resembles the Huygens principle, a well-known theory from classical physics of waves. According to it, each scattering center (point) is a source of an independent spherical wave. These waves add together giving rise to an interference pattern.

Using an explicit form of the one-particle Green's function in three dimensions (Eq. (6)) and approximating the t-matrix by an effective scattering length $b_i^{\rm scatt}=\lim_{k\to 0}f_i^+(k)$, where $\hbar\omega=\hbar^2k^2/2m$ and $f_i^+(k)$ is the scattering amplitude due to the $i^{\rm th}$ impurity and obtained directly from the t-matrix $T_{ii}(\omega)$, we find that the change in the particle density is expressed by

$$\Delta n(\boldsymbol{r})=\sum_{i=1}^{N_{\rm imp}}I_i^{\rm scatt}\frac{(2k_{\rm F}|\boldsymbol{r}-\boldsymbol{l}_i|)\cos(2k_{\rm F}|\boldsymbol{r}-\boldsymbol{l}_i|)-\sin(2k_{\rm F}|\boldsymbol{r}-\boldsymbol{l}_i|)}{(2k_{\rm F}|\boldsymbol{r}-\boldsymbol{l}_i|)^4}\,, \tag{25}$$

where $I_i^{\rm scatt}\sim b_i^{\rm scatt}$ are constants depending on the impurity potential strengths V_i [24]. In the asymptotic limit $|\boldsymbol{r}-\boldsymbol{l}_i|\gg 1/k_{\rm F}$, we obtain a generalization of the Friedel result to the multiple impurities case

$$\Delta n(\boldsymbol{r})=\sum_{i=1}^{N_{\rm imp}}I_i^{\rm scatt}\frac{\cos(2k_{\rm F}|\boldsymbol{r}-\boldsymbol{l}_i|)}{(2k_{\rm F}|\boldsymbol{r}-\boldsymbol{l}_i|)^3}\,. \tag{26}$$

In the dilute limit, one expects that the FO pattern is a sum of FO patterns yielded by each independent impurity. The oscillatory behavior decays as the cubic distance from the impurities. In Fig. 3, we plot the results for FO based on the generalized formula (26) in the case of two impurities in three dimensions and compare them with the exact results. The ω dependence of the diagonal t-matrix elements seems to be relevant is space between the impurities. However, outside the impurities, Eq. (26) practically describes FO from two impurities very well.

In a similar way, one can obtain the generalization of the Friedel result in two dimensions

$$\Delta n(\boldsymbol{r})=\sum_{i=1}^{N_{\rm imp}}I_i^{\rm scatt}\frac{\sin(2k_{\rm F}|\boldsymbol{r}-\boldsymbol{l}_i|)}{(2k_{\rm F}|\boldsymbol{r}-\boldsymbol{l}_i|)^2}\,. \tag{27}$$

The last result required an asymptotic form of the Green's function in two dimensions, which is found from an asymptotic expansion of the Hankel function $H_\nu^+(z) \approx \sqrt{2/\pi z}\exp[i(z-(2\nu+1)\pi/4)]$. The oscillatory behavior decays as the square distance from the impurities.

Finally, we note that a superposition of FO from independent impurities gives rise to the interference patterns. A few cases, determined from Eq. (27) for multiple impurities in two dimensions, are shown in Fig. 4. We

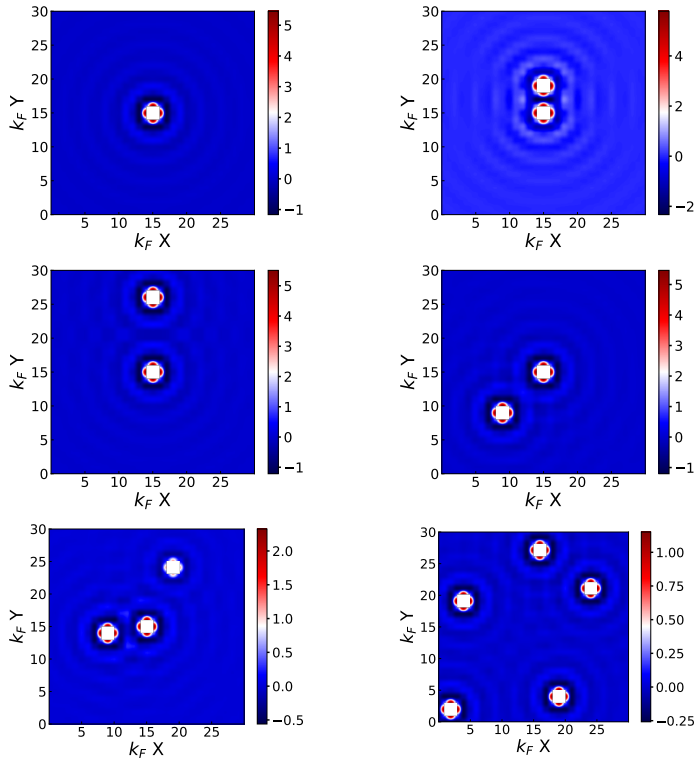

Fig. 4. The Friedel oscillations and interference patterns in the two-dimensional system of non-interacting fermions. Upper left panel: A single impurity with $I_1 = 24$ placed at $\boldsymbol{l}_1 = (16, 16)$. Upper right panel: Two impurities close to each other with $I_1 = I_2 = 24$ placed at $\boldsymbol{l}_1 = (16, 16)$ and $\boldsymbol{l}_2 = (16, 20)$. Middle left panel: Two impurities far away from each other with $I_1 = I_2 = 24$ placed at $\boldsymbol{l}_1 = (16, 16)$ and $\boldsymbol{l}_2 = (16, 27)$. Middle right panel: Two impurities placed diagonally with $I_1 = I_2 = 24$ placed at $\boldsymbol{l}_1 = (10, 10)$ and $\boldsymbol{l}_2 = (16, 16)$. Lower left panel: Three impurities with different strengths $I_1 = 10$ at $\boldsymbol{l}_1 = (16, 16)$, $I_2 = 10$ at $\boldsymbol{l}_1 = (10, 15)$, and $I_3 = 5$ at $\boldsymbol{l}_3 = (20, 25)$. Lower right panel: Multiple impurities with $I_{i=1,\ldots,5} = 5$ and at positions $\boldsymbol{l}_1 = (3, 3)$, $\boldsymbol{l}_2 = (20, 5)$, $\boldsymbol{l}_3 = (5, 20)$, $\boldsymbol{l}_4 = (25, 22)$, and $\boldsymbol{l}_5 = (17, 28)$. Here, the uniform density of particles is set by $k_\mathrm{F} = 1$, which leads to a characteristic wavelength scale $\lambda_\mathrm{F} = 2\pi/k_\mathrm{F} \approx 6$.

selected the phase shifts $\phi_i = 0$ for each impurity and $k_F = 1$, which sets a characteristic wavelength scale $\lambda_F = 2\pi/k_F$. Hence, the uniform density of particles is different from that in Section 3. The presented patterns resemble those seen in various STM experiments on metallic surfaces with subsurface defects or impurities [25].

5. Conclusions

In this paper, we revisited the problem of scattering off a few localized impurities and analyzed analytically and numerically the behavior of the particle density oscillations. The relevance of the diagonal and off-diagonal elements of the t-matrix was discussed. When the distance between impurities is large, compared to the Fermi wavelength, the role of the off-diagonal matrix elements of the t-matrix is negligible. Then, following the Huygens principle, one can view an interference pattern as a sum of independent waves in the density profiles — a sum of Friedel oscillations. The generalized Friedel's formula due to many impurities was derived.

This superposition principle holds for the density oscillations, not true waves, and is valid only if distances between impurities and the point of observation are large. Nevertheless, this is an interesting and perhaps practical result that would help to analyze STM images seen experimentally. It would be exciting to check if, for example, quantum mirage can be seen within our generalized Friedel formula, when applied to quantum corrals. Further developments of our finding toward the Kondo effect for fermions scattered off a few magnetic impurities is also a requested topic for the future.

On the occasion of the scientific jubilee of Professor Józef Spałek, the authors would like to congratulate him on his wonderful achievements in theoretical physics and in the theory of strongly correlated electron systems, and to wish him many more years of further successes in physics, as well as good health and prosperity in his life.

REFERENCES

[1] J. Friedel, «XIV. The distribution of electrons round impurities in monovalent metals», *Phil. Mag.* **43**, 153 (1952).

[2] J. Friedel, «Metallic alloys», *Nuovo Cim. Supp.* **7**, 287 (1958).

[3] C. Kittel, «Quantum Theory of Solids», *John Wiley& Sons, Inc.*, New York, London, Sidney 1963.

[4] J. Villain, M. Lavagna, P. Bruno, «Jacques Friedel and the physics of metals and alloys», *C. R. Physique* **17**, 276 (2016).

[5] É. Daniel, «How the Friedel oscillations entered the physics of metallic alloys», *C. R. Physique* **17**, 291 (2016).

[6] C. Benta, «Friedel oscillations: Decoding the hidden physics», *C. R. Physique* **17**, 302 (2016).

[7] A. Georges, «The beauty of impurities: Two revivals of Friedel's virtual bound-state concept», *C. R. Physique* **17**, 430 (2016).

[8] G. Binnig, H. Rohrer, Ch. Gerber, E. Weibl, «Tunneling through a controllable vacuum gap», *Appl. Phys. Lett.* **40**, 178 (1982); «Surface Studies by Scanning Tunneling Microscopy», *Phys. Rev. Lett.* **49**, 57 (1982); «7 × 7 Reconstruction on Si(111) Resolved in Real Space», *ibid.* **50**, 120 (1983).

[9] S. Lounis, «Theory of scanning tunneling microscopy», arXiv:1404.0961 [cond-mat.mes-hall].

[10] D.M. Eigler, E.K. Schweizer, «Positioning single atoms with a scanning tunnelling microscope», *Nature* **344**, 524 (1990).

[11] M.F. Crommie, C.P. Lutz, D.M. Eigler, «Confinement of Electrons to Quantum Corrals on a Metal Surface», *Science* **262**, 218 (1993).

[12] E.J. Heller, M.F. Crommie, C.P. Lutz, D.M. Eigler, «Scattering and absorption of surface electron waves in quantum corrals», *Nature* **369**, 464 (1994).

[13] H.C. Manoharan, C.P. Lutz, D.M. Eigler, «Quantum mirages formed by coherent projection of electronic structure», *Nature* **403**, 512 (2000).

[14] K. Kanisawa, M. Butcher, H. Yamaguchi, Y. Hirayama, «Imaging of Friedel Oscillation Patterns of Two-Dimensionally Accumulated Electrons at Epitaxially Grown InAs(111) *A* Surfaces», *Phys. Rev. Lett.* **86**, 3384 (2001).

[15] Y. Hasegawa *et al.*, «Real-Space Observation of Screened Potential and Friedel Oscillation by Scanning Tunneling Spectroscopy», *J. Phys.: Conf. Ser.* **61**, 399 (2007).

[16] G.A. Fiete, E.J. Heller, «*Colloquium*: Theory of quantum corrals and quantum mirages», *Rev. Mod. Phys.* **75**, 933 (2003).

[17] E.N. Economou, «Green's Functions in Quantum Physics» Springer Series in Solid-State Sciences, *Springer-Verlag*, Berlin, Heidelberg 2006.

[18] M. Abramowitz, I.A. Stegun, «Handbook of Mathematical Functions», *Dover*, London 1974.

[19] E. Fermi, «Sul moto dei neutroni nelle sostanze idrogenate», *Ric. Sci.* **7**, 13 (1936).

[20] K. Wódkiewicz, «Fermi pseudopotential in arbitrary dimensions», *Phys. Rev. A* **43**, 68 (1991).

[21] B. Donner, M. Kleber, C. Bracher, H.J. Kreuzer, «A simple method for simulating scanning tunneling images», *Am. J. Phys.* **73**, 690 (2005).

[22] T.T. Le *et al.*, «Generalization of the Fermi pseudopotential», *Phys. Scr.* **94**, 065203 (2019).

[23] K. Huang, «Statistical Mechanics», *John Wiley and Sons, Inc.*, New York 1963.

[24] F. García-Molinear, «Quantum-mechanical techniques», in: «Theory of Imperfect Crystalline Solids: Trieste Lectures 1970», *International Atomic Anergy Agency*, Vienna 1971, pp. 1–100.

[25] A. Weismann *et al.*, «Seeing the Fermi Surface in Real Space by Nanoscale Electron Focusing», *Science* **323**, 1190 (2009).